Photoactive oriented films of layered double hydroxides

Kamil Lang,*[a] Pavel Kubát,[b] Jiří Mosinger,[ac] Juraj Bujdák,[d] Martin Hof,[b] Pavel Janda,[b] Jan Sýkora[b] and Nobuo Iyi[e]

Received 26th March 2008, Accepted 13th May 2008
First published as an Advance Article on the web 18th June 2008
DOI: 10.1039/b805081c

The treatment of nano-ordered oriented films of layered double hydroxide (LDH) with dodecyl sulfate increased the interlayer distance from 0.4 to 1.96 nm, which allowed the intercalation of 5,10,15,20-tetrakis(4-sulfonatophenyl)porphyrin (TPPS). The re-stacking of separated layers and the rebuilding of crystals oriented parallel to the surface of quartz slides was confirmed by X-ray diffraction and atomic force microscopy. The hybrid films contained homogeneously distributed porphyrin molecules with preserved photophysical properties such as fluorescence, triplet state formation, and energy transfer, thus forming singlet oxygen.

Introduction

The controlled organization of photoactive molecules, *e.g.*, porphyrins, in films offers numerous prospective applications ranging from catalysis and photosensitized oxygenation to the immobilization of biomaterials or nonlinear optics.[1–4] The photophysical properties of nanoscaled layers are mainly determined by the extent of an ordered molecular arrangement, the orientation of the photoactive moieties, the distance between them, and the orientation between photoactive moieties and incident radiation.[5]

In self-assembled films, porphyrin molecules are closely stacked; therefore, excitation energy can be transferred among them due to electronic interactions.[1] During the preparation of photofunctional materials, these interactions, which lead to molecular aggregation, should be suppressed because they open new competitive channels for energy dissipation.[6] The dissipation of energy causes a significant decrease in the excited state lifetimes and competes with all photoinduced reactions. A technique to prevent aggregation is to immobilize individual molecules in the solids using ordered structures such as zeolites, clays, and layered double hydroxides (LDH).[7–9] The advantages of this technique are the defined microscopic structures of host matrices and the specific organization, high variability, and stability of photoactive molecules.

The structure of LDH (Fig. 1) can be described as a stack of positively charged metal hydroxide layers with counter anions and water molecules placed in the interlayer space.[10] The ordering of hydroxide layers is similar to that of brucite, $Mg(OH)_2$, where each Mg^{2+} cation is octahedrally surrounded by six OH^- anions and the resulting octahedra share edges to form infinite sheets. The isomorphous substitution of M^{II} by M^{III} results in a net positive charge, which is neutralized by interlayer anionic species. The binding of monovalent anions in the interlayer space is relatively weak. Therefore, the anion exchange procedure can produce LDH intercalated with desired anions. The chemical composition of LDH is represented by the general formula $[M^{II}_{1-x}M^{III}_x(OH)_2]^{x+}[A^{n-}_{x/n}\cdot yH_2O]^{x-}$, where M^{II} and M^{III} are divalent and trivalent metal ions, A^{n-} is the counter anion, and x usually varies between 0.20 and 0.35. A large variety of hybrid materials can be prepared by varying metal cations, compensating anions, and layer charge density through controlling the ratio x.

Recently, we have described the structural and photophysical properties of LDH powders with intercalated porphyrin sensitizers in which the porphyrin plane is nearly perpendicular to the hydroxide layers.[9] It has been shown that the properties of porphyrin triplet states are not critically altered by the surrounding matrix as these states rapidly interact with oxygen molecules by energy transfer, thus forming singlet oxygen $O_2(^1\Delta_g)$.

A nonphotochemical generation of $O_2(^1\Delta_g)$ by the catalyzed decomposition of hydrogen peroxide by molybdate- and tungstate-LDH hybrids can be suitable for large-scale applications in the dark.[11] The presented LDH hybrides with intercalated porphyrin sensitizers convert oxygen in the ground state, *i.e.*, $O_2(^3\Sigma_g)$, to reactive $O_2(^1\Delta_g)$; an example of the application of such hybrids is the construction of bactericidal surfaces. This concept would be more effective when photoactive coatings

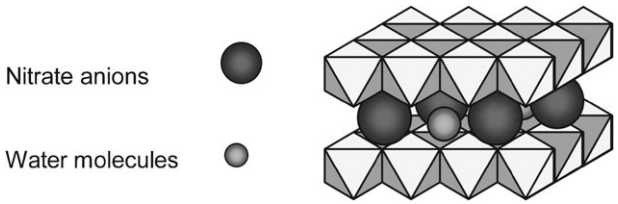

Fig. 1 Structure of $[Mg_4Al_2(OH)_{12}]^{2+}$ layers.

[a] *Institute of Inorganic Chemistry, v.v.i., Academy of Sciences of the Czech Republic, 250 68 Řež, Czech Republic. E-mail: lang@iic.cas.cz; Fax: +420 220 941 502; Tel: +420 266 172 193*
[b] *J. Heyrovský Institute of Physical Chemistry, v.v.i., Academy of Sciences of the Czech Republic, Dolejškova 3, 182 23 Praha 8, Czech Republic. E-mail: kubat@jh-inst.cas.cz*
[c] *Faculty of Sciences, Charles University in Prague, Hlavova 2030, 128 43 Praha 2, Czech Republic*
[d] *Institute of Inorganic Chemistry, Slovak Academy of Sciences, Dúbravská cesta 9, 845 36 Bratislava, Slovakia*
[e] *Nanoscale Materials Center, National Institute of Materials Science (NIMS), 1-1 Namiki, Tsukuba, 305-0044, Japan*

are used instead of powders. We now report the fabrication and characterization of well-defined films that utilize the photoactive properties of oriented porphyrin molecules, which, to the best of our knowledge, is being reported for the first time.

Experimental

Materials

The tetrasodium salt of 5,10,15,20-tetrakis(4-sulfonatophenyl)porphyrin (TPPS) (Aldrich), $Al(NO_3)_3{\cdot}9H_2O$, $Mg(NO_3)_2{\cdot}6H_2O$ and NaOH (all manufactured by Penta, Czech Republic), and sodium dodecylsulfate (DDS, Merck) were used as received.

Sample preparation. The LDH host in the nitrate form was prepared by coprecipitation according to a method by Miyata.[12] Carbonate-free distilled water and nitrogen atmosphere were employed to avoid the contamination of the final product by carbonate anions. Aqueous solutions of $Mg(NO_3)_2{\cdot}6H_2O$ and $Al(NO_3)_3{\cdot}9H_2O$ (450 ml, molar ratio Mg/Al = 2, total metal ion concentration = 1.0 M) were added to a reactor containing 200 ml of distilled water at a flow rate of 7.5 ml min^{-1}. Simultaneously, an aqueous solution of NaOH (3 M) was also added to maintain the pH value of the mixture at a constant value of 10.0 ± 0.1. Coprecipitation was carried out under vigorous stirring at 75 °C, and the resulting suspension was further stirred for 1 h at this temperature. The product was filtered off, washed several times with distilled water, and dried at 60 °C.

Preparation of films. The DDS/LDH films were treated with 10^{-5} M aqueous solution of TPPS at room temperature. Some hybrid films were prepared by the treatment of unmodified LDH with TPPS at room temperature or with a mixture solution containing TPPS and DDS at 60 °C for 3 h.

Methods and instrumentation

X-Ray diffraction (XRD). The diffraction patterns of synthesized original LDH and organo-LDH were recorded from 2 to 30°/2θ with a step size of 0.01° using a RINT 1200 diffractometer (Rigaku) at room temperature (continuous scanning type) and a Dmax 1000 horizontal goniometer (scanning speed 2° min^{-1}, Ni-filtered Cu Kα radiation: 40 kV, 30 mA).

Absorption spectroscopy. The UV/Vis absorption spectra of the hybrid films were recorded using a PerkinElmer Lambda 35 spectrometer.

Steady-state fluorescence. The fluorescence spectra were measured on a PerkinElmer LS 50B luminescence spectrophotometer. All fluorescence emission spectra were corrected for the characteristics of a detection monochromator and photomultiplier by using fluorescence standards. The samples were excited to the Soret (417 nm) and Q_y(1,0) (513 nm) absorption bands.

Time-resolved fluorescence. The fluorescence decay curves were recorded on a 5000U single photon counting setup (IBH, Glasgow, UK) using an IBH laser diode NanoLED-440L (440 nm peak wavelength, pulse width < 200 ps, 1 MHz maximum repetition rate) and a cooled Hamamatsu R3809U-50 microchannel plate photomultiplier. The decay curves were recorded at 660 nm. Additionally, a 550 nm cut-off filter was used to eliminate scattered light. The data were collected until the peak value reached 10 000 counts. The decay curves were fitted to multiexponential functions (one, two or three exponential components were used) using an iterative reconvolution procedure of the IBH DAS6 software.

Laser flash photolysis. Laser flash photolysis experiments were performed using a Lambda Physik FL 3002 dye laser (425 nm, output < 2 mJ $pulse^{-1}$) pumped with a Lambda Physik Compex 102 excimer laser (308 nm, pulse width 28 ns). Transient spectra (435–540 nm) were recorded using an LKS 20 laser kinetic spectrometer (Applied Photophysics, UK). The time profiles of the triplet state decay were recorded at 450 nm using an R928 photomultiplier (Hamamatsu) and a 250 W Xe lamp equipped with a pulse unit. The lifetimes of the porphyrin triplet states were obtained by exponential fitting to decay curves measured in air, argon, or oxygen atmosphere. The equilibration of the films in a given atmosphere was carried out by purging the cell where the quartz slides were placed with Ar or O_2 for at least 30 min.

Singlet oxygen luminescence. The time-resolved near-infrared luminescence of $O_2(^1\Delta_g)$ at 1270 nm was monitored using a home-made detector (1270 nm interference filter, Judson J16-8SP-R05M-HS Ge diode) upon laser excitation by a Lambda Physik FL 3002 dye laser (λ_{exc} = 425 nm, incident energy 0.1–0.2 mJ $pulse^{-1}$). The signal from the detector was collected in a 600 MHz oscilloscope (Agilent Infiniium) and transferred to a computer for further analysis. The signal-to-noise ratio of the signals was improved by the averaging of 100 to 1000 individual traces. The short-lived signal produced by the scattering of an excitation laser pulse and/or by red fluorescence could be eliminated by exciting the sample in argon atmosphere and by subtracting the obtained signal from the signal recorded in oxygen atmosphere.[9] The equilibration of the films in a given atmosphere was carried out by purging the cell where the quartz slides were placed with Ar or O_2 for at least 30 min.

Atomic force microscopy (AFM). The modified LDH films were imaged by an atomic force microscope (TopoMetrix model Discoverer, Veeco, USA) in contact, lateral force, and force modulation (dF/dz) modes. A standard SFM Probes Model 1520-00 (Veeco, USA) was used. While the three-dimensional size of the nanostructures was visualized in the contact mode, the lateral and semicontact force modulation techniques yielded high-resolution grain boundary images.

Confocal fluorescence microscopy and fluorescence lifetime imaging microscopy (FLIM). Confocal fluorescence microscopy and FLIM were carried out using a MicroTime 200 inverted epifluorescence confocal microscope (PicoQuant, Germany). We used a configuration comprising a pulsed diode laser (LDH-P-C-405, 405 nm, PicoQuant) providing 80 ps pulses at a repetition rate of 40 MHz, a 505DRLP dichroic mirror, an LP500 (Omega Optical) long-pass filter, water

immersion objective (1.2 NA, 60×) (Olympus), and a PDM SPAD detector (MPD, USA). A PicoHarp 300 module (PicoQuant, Germany) recorded photon events in a TTTR mode, enabling the reconstruction of the lifetime histogram for each pixel.[13] A low power of 1.5 μW at the back aperture of the objective was selected in order to minimize pile-up effects. The data were analyzed using the OriginPro70 software package (OriginLab Corp., MA, USA).

Results and discussion

Synthesis and XRD analysis

The LDH powder with the theoretical formula $Mg_4Al_2(OH)_{12}(NO_3)_2{\cdot}4H_2O$ (Fig. 1) was synthesized using the coprecipitation method[9] and delaminated by formamide.[14–16] The measured ratio of Mg/Al was 2.27.[9] The resulting gel was cast on quartz slides and dried at 90 °C to remove the solvent. The complete restacking of the separated layers and the rebuilding of the crystals oriented parallel to the surface of the quartz slides with NO_3^- ions as compensating ions were confirmed by XRD (Fig. 2a).

The DDS/LDH hybrid films were prepared by the treatment of the LDH films with a 10^{-3} M DDS aqueous solution at 60 °C for 3 h. These conditions allowed the complete saturation by DDS. The XRD patterns indicated that surfactant molecules were intercalated in the LDH galleries because of a progressive increase in the basal spacing d_{003} from 0.88 to 2.44 nm (Fig. 2a and b). Taking into account the thickness of the LDH layer (0.48 nm), the interlayer distance increased from 0.4 nm, corresponding to the space occupied by the nitrate anions, to 1.96 nm. This modification increased the internal space and converted the essentially hydrophilic internal surface into one that was hydrophobic and capable of accommodating relatively large molecules with hydrophobic aromatic units. This distance indicated that the DDS alkyl chains were tilted away from the interlamellar normal and not perpendicularly arranged with respect to the hydroxide layer.[17,18] A comparison of the XRD pattern of the original LDH film with that of the hybrid films revealed that the hybrid

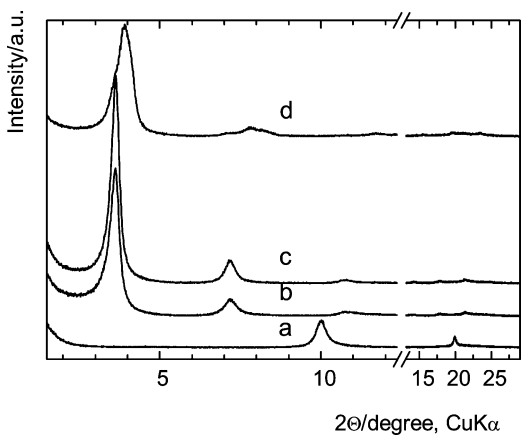

Fig. 2 Diffraction patterns of the original nitrate form of LDH (a), DDS/LDH (b), DDS/LDH after treatment with 10^{-5} M TPPS for 10 min (c), and DDS/LDH after treatment with 10^{-5} M TPPS for 3 days (d). The patterns are offset for clarity.

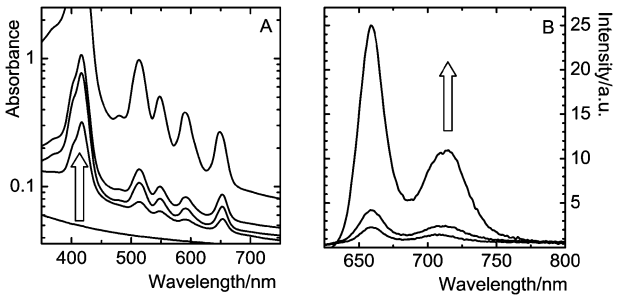

Fig. 3 UV/Vis absorption spectra of DDS/LDH films deposited on a quartz slide after treatment with 10^{-5} M TPPS for 10 min, 1 h, 2.5 h and 3 days, the bottom spectrum is for the reference DDS/LDH film without TPPS (A); corresponding fluorescence emission spectra after treatment for 30 min, 1 h and 2.5 h, for excitation to 513 nm (B). The arrows show changes with increasing treatment time.

films had a more ordered structure, as shown by the increased intensity of the diffraction lines in the XRD pattern. The DDS/LDH films were further treated with a 10^{-5} M aqueous solution of TPPS at room temperature. The progression of TPPS absorption and fluorescence emission spectra verified that TPPS had high affinity towards the LDH layers (Fig. 3). Intercalation is a relatively slow process and the most loaded films are obtained after being treated for three days. Fairly small changes in the XRD patterns indicate that the lamellar structure of the films is maintained (Fig. 2). We suppose that the porphyrin molecules can be partially exchanged with DDS anions or occupy cavities within the hydrophobic DDS phase. The greatest change occurs after a three-day sorption because d_{003} decreases from 2.44 to 2.29 nm (Fig. 2d). Evidently, as more DDS molecules are exchanged with TPPS, d_{003} approaches a value typical of a pure TPPS/LDH hybrid.[9] It should be mentioned that the hybrid films prepared by the treatment of unmodified LDH with TPPS or mixed solutions of TPPS and DDS have disordered structures with a small fraction of the intercalated phase.

UV/Vis absorption and emission spectra

The intercalation of TPPS between the LDH layers is monitored by absorption (Fig. 3A) and fluorescence spectroscopies (Fig. 3B). The intensity of the absorption bands increases with an increase in the contact time of the DDS/LDH films with the TPPS solution. These results complement the XRD observations and show the importance of the contact time for obtaining heavily loaded hybrids. In addition, the shape of the Soret band is a sensitive diagnostic tool for porphyrin molecular packing. Upon binding, the Soret band is broadened and slightly red-shifted from 413 nm (Fig. 4a) to 416 nm (Fig. 4b). We attribute these spectral effects to the contribution of a range of binding sites in the LDH matrix and to possible nonplanar deformations of the porphyrin units upon intercalation.[19] The absence of distinct splitting and the presence of a small spectral shift in the Soret band rule out extensive porphyrin aggregation within the LDH interspace, a process that occurs in solutions and on solid templates.[20,21]

The extensive aggregation of TPPS progresses in the untreated LDH films, as indicated by the blue shift of the Soret bands to 407 nm (Fig. 4c) and by poor fluorescence properties.

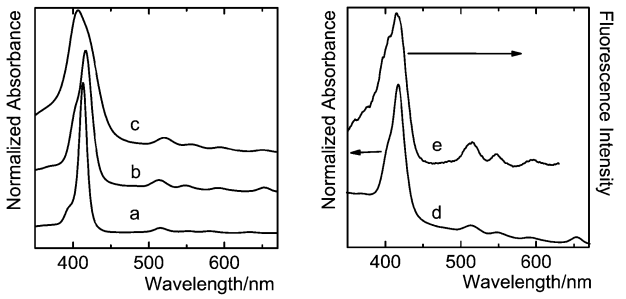

Fig. 4 UV/Vis absorption spectra of TPPS in aqueous solution (a), in the hybrid film prepared *via* intercalation in a DDS/LDH film (b), and in the film prepared *via* sorption of TPPS into original nitrate LDH at 65 °C for 1 h (c). Comparison of absorption (d) and fluorescence excitation spectra (e) of the DDS/LDH film after its treatment with a 10^{-5} M TPPS for 10 min (emission observed at 658 nm). All spectra are offset for clarity.

Aggregation is an undesired process due to the rapid dissipation of absorbed energy mediated by exciton coupling between the stacked porphyrin units. Competitive relaxation reduces the fluorescence lifetimes and quantum yields and suppresses the formation of the porphyrin triplet states.[6]

The intensity of the fluorescence emission spectra is an important indicator of the porphyrin molecular form (monomer *vs.* aggregate) and photoactivity. Two emission bands are located at 659 and 714 nm; however, the positions vary slightly depending on the conditions of the porphyrin loading (Fig. 3B). A comparison of the absorption (Fig. 4d) and fluorescence excitation spectra (Fig. 4e) confirms that the porphyrin molecules are the only photoactive components.

To investigate the relaxation of the excited singlet states of TPPS, the fluorescence time profiles are analysed. TPPS has a lifetime of 9.6 ns.[22] Adequate fits to the fluorescence kinetics of the hybrid materials require two or three exponential functions; the lifetime of TPPS generally decreases ($\sim$1.5 ns and $\sim$6 ns, respectively). Surprisingly, increased loading leads to the appearance of a long-lived component at $\sim$9 ns (*e.g.*, DDS/LDH after treatment with 10^{-5} M TPPS for 3 d has components of 0.67 ns (11%), 2.90 ns (38%), and 9.24 ns (51%)). If TPPS aggregates the excited singlet lifetime should be very short, but the results showed this not to be true. The existence of several lifetimes, therefore, stems from the interaction between the porphyrin molecules and the host matrix: (i) the presence of different binding sites can lead to distinct types of singlet state decay kinetics; (ii) the strong interaction of the porphyrin molecules with the matrix may result in a conformational deformation of the porphyrin ring and, as a consequence, to the population of differently decaying singlet states. The porphyrin molecules in LDH have singlet lifetimes sufficiently long to undergo photochemical reactions. The high intensities of the fluorescence emission, well-resolved fluorescence emission peaks, and contribution of the long-lived fluorescence component are the properties because of which we further focus on the photophysics of highly loaded TPPS/DDS/LDH films.

AFM

The semicontact force modulation AFM image reveals a compact nanostructure composed of nanoparticles lying parallel to the quartz surface (Fig. 5). It confirms the XRD results. The lateral size of the nanostructures found in the deposited films is of the order of hundreds of nanometers. The thickness measured between the overlapping nanoparticles at several locations was between 16 and 25 nm. The theoretical thickness of the LDH sheet is 0.48 nm and the interlayer distance is close to 2 nm; therefore, the analyzed particles are composed of approximately 10 LDH layers.

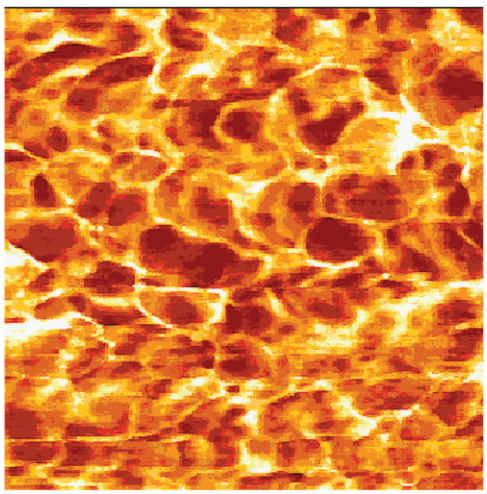

Fig. 5 AFM force modulation image (1 × 1 μm) of the DDS/LDH film after treatment with 10^{-5} M TPPS for 2.5 h.

Confocal fluorescence microscopy and FLIM

The use of fluorescence microscopy leads to new and important insights into the spatial distribution of anion-exchange sites throughout LDH crystals.[23] After determining the integral fluorescence properties, we apply confocal fluorescence microscopy to specify the fluorescence intensity (Fig. 6a and b) and lifetime distributions (Fig. 6c and d) in the bulk of the hybrid films on the quartz surface. There are no low-intensity regions that could indicate the aggregation of the porphyrin molecules and competitive nonradiative processes. The *z*-scan shows several high-intensity spots that can be explained through the presence of highly concentrated areas of the photoactive porphyrin units in the matrix bulk (Fig. 6a). The thickness of the fluorescent film is 4.7 ± 0.2 μm. The spatial arrangement and/or distribution of the porphyrin fluorophore are relatively homogeneous with no indication of porphyrin aggregation within the microscope resolution (lateral $\sim$250 nm).

To characterize the fluorescence decay recorded for each pixel, the average lifetimes are calculated as $\tau_{av} = \Sigma I_i t_i / \Sigma I_i$, where I_i and t_i are the intensity and time corresponding to the ith channel, respectively. The average lifetime image (Fig. 6c) shows homogeneity similar to that observed in the intensity measurements. The average lifetime distribution corresponds to the Gaussian distribution model, yielding a mean lifetime of 2.30 ± 0.01 ns (Fig. 6d).[24]

Triplet states and singlet oxygen

The films are investigated by laser flash photolysis in order to characterize the excited-state dynamics of the intercalated TPPS

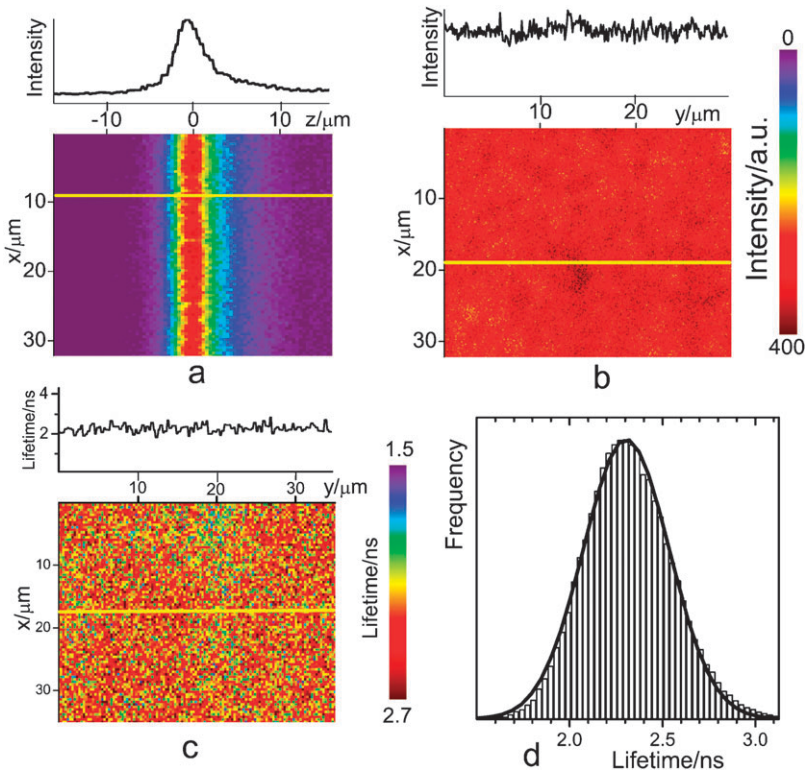

Fig. 6 Fluorescence intensity images of the DDS/LDH film after treatment with 10^{-5} M TPPS for 1.5 h: z scan (a) and x–y scan at $z = 0$ (b). Corresponding average lifetime image for the x–y scan at $z = 0$ (c) and distribution of the average lifetimes (the solid line is the Gaussian fit to the data) (d). The upper panels show the intensities along the marked lines; the film is excited at 405 nm and emission is collected above 450 nm.

molecules. The transient difference absorption spectra show the typical features of the porphyrin triplet states in solution, *i.e.*, a broad positive absorption band within 435–550 nm arising from triplet–triplet absorption. The transient has a lifetime of greater than 600 μs (Fig. 7A), and its decay is accelerated by oxygen (lifetimes of 10.0 and 5.1 μs in air and O_2, respectively), which supports the transient assignment to the porphyrin triplet states. A comparison of these triplet lifetimes with the lifetimes of TPPS in aqueous solution (414 μs in oxygen-free water and 2 μs in air-saturated water, *i.e.*, at 0.28 mM O_2)[25] shows that the host matrix suppresses quenching by O_2. This can be explained by the slower diffusion of O_2 in the films.

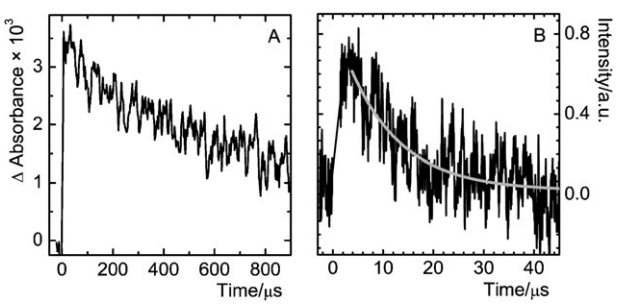

Fig. 7 Decay of triplet states of TPPS intercalated in the DDS/LDH film after treatment with 10^{-5} M TPPS for 3 d ($\lambda_{exc} = 425$ nm, $\lambda_{obs} = 450$ nm, energy <1 mJ, averaging of 30 individual traces) in argon atmosphere (A). Time dependence of the $O_2(^1\Delta_g)$ luminescence signal at 1270 nm. The smoothed gray line is a least squares monoexponential fit (B).

In contrast to TPPS intercalated in LDH powders having multiexponential decay kinetics,[9] in the films, the triplet states are fairly fitted with a monoexponential function. Evidently, all the generated triplet states are equivalent with respect to quenching by O_2. These observations clearly demonstrate that the porphyrin molecules can be effectively excited to the triplet states and that these states are accessible to oxygen molecules even when TPPS is placed within the interlayer space of the LDH films.

Although the production of $O_2(^1\Delta_g)$ can be predicted on the basis of the transient absorption measurements, direct evidence for energy transfer is obtained from the time-dependent luminescence at 1270 nm. Fig. 7B depicts the $O_2(^1\Delta_g)$ luminescence recorded after the laser excitation of TPPS in the film. Since pure LDH films do not exhibit any $O_2(^1\Delta_g)$ luminescence, we conclude that $O_2(^1\Delta_g)$ is generated solely by the porphyrin photosensitized reaction. The $O_2(^1\Delta_g)$ lifetimes recovered from the monoexponential fits (10 μs) are comparable to the lifetimes of the precedent porphyrin triplet states, indicating that the $O_2(^1\Delta_g)$ decay kinetics predominantly reflect the duration of the triplet states. For comparison, the $O_2(^1\Delta_g)$ lifetimes in the LDH powders vary within 6–64 μs.[9] The lifetimes are probably affected by Mg- and Al-coordinated OH groups oriented toward the interlayer space and also by confined water molecules. We are currently exploring materials with longer $O_2(^1\Delta_g)$ lifetimes.

Conclusion

In summary, oriented LDH films with intercalated TPPS molecules combine the advantages of the nano-ordered and

tunable structure of LDH with the photophysical properties of TPPS. The presented results contribute to the understanding of the singlet oxygen production channels and reactivity in solid-state matrices.

Acknowledgements

The authors gratefully acknowledge financial support from the Czech Science Foundation (No. 203/06/1244), the APVV agency (No. 027 405, to J.B.), and from VEGA 2/6180/27 (to J.B.).

References

1. H. Donker, A. van Hoek, W. van Schaik, R. B. M. Koehorst, M. M. Yatskou and T. J. Schaafsma, *J. Phys. Chem. B*, 2005, **109**, 17038.
2. M. Ogawa and K. Kuroda, *Chem. Rev.*, 1995, **95**, 399.
3. S. Takagi, D. A. Tryk and H. Inoue, *J. Phys. Chem. B*, 2002, **106**, 5455.
4. S. Takagi, M. Eguchi, D. A. Tryk and H. Inoue, *J. Photochem. Photobiol., C*, 2006, **7**, 104.
5. G. Schulz-Ekloff, D. Wöhrle, B. van Duffel and R. A. Schoonheydt, *Microporous Mesoporous Mater.*, 2002, **51**, 91.
6. K. Lang, J. Mosinger and D. M. Wagnerová, *Coord. Chem. Rev.*, 2004, **248**, 321.
7. S. Bonnet, C. Forano, A. de Roy, J. P. Besse, P. Maillard and M. Momenteau, *Chem. Mater.*, 1996, **8**, 1962.
8. F. Leroux and C. Taviot-Guého, *J. Mater. Chem.*, 2005, **15**, 3628.
9. K. Lang, P. Bezdička, J. L. Bourdelande, J. Hernando, I. Jirka, E. Káfuňková, F. Kovanda, P. Kubát, J. Mosinger and D. M. Wagnerová, *Chem. Mater.*, 2007, **19**, 3822.
10. D. G. Evans and R. C. T. Slade, in *Layered Double Hydroxides*, ed. X. Duan and D. G. Evans, Springer-Verlag, Berlin, Heidelberg, 2006, Struct. Bond. 119, p. 1.
11. B. F. Sels, D. E. De Vos and P. A. Jacobs, *J. Am. Chem. Soc.*, 2007, **129**, 6916.
12. S. Miyata, *Clays Clay Miner.*, 1975, **23**, 369.
13. P. Kapusta, M. Wahl, A. Benda, M. Hof and J. Enderlein, *J. Fluoresc.*, 2007, **17**, 43.
14. L. Li, R. Ma, Y. Ebina, N. Iyi and T. Sasaki, *Chem. Mater.*, 2005, **17**, 4386.
15. Q. Wu, A. Olafsen, O. B. Vistad, J. Roots and P. Norby, *J. Mater. Chem.*, 2005, **15**, 4695.
16. K. Okamoto, T. Sasaki, T. Fujita and N. Iyi, *J. Mater. Chem.*, 2006, **16**, 1608.
17. L. Mohanambe and S. Vasudevan, *J. Phys. Chem. B*, 2006, **110**, 14345.
18. H. Zhao and K. L. Nagy, *J. Colloid Interface Sci.*, 2004, **274**, 613.
19. R. E. Haddad, S. Gazeau, J. Pécaut, J.-C. Marchon, C. J. Medforth and J. A. Shelnutt, *J. Am. Chem. Soc.*, 2003, **125**, 1253.
20. P. Kubát, K. Lang, K. Procházková and P. Anzenbacher, *Langmuir*, 2003, **19**, 422.
21. W. Xu, H. Guo and D. L. Akins, *J. Phys. Chem. B*, 2001, **105**, 1543.
22. P. Kubát, K. Lang and P. Anzenbacher, *Biochim. Biophys. Acta*, 2004, **1670**, 40.
23. M. B. J. Roeffaers, B. F. Sels, D. Loos, Ch. Kohl, K. Mullen, P. A. Jacobs, J. Hofkens and D. E. De Vos, *ChemPhysChem*, 2005, **6**, 2295.
24. The lifetime obtained by the FLIM method differs from the values gained by the standard TCSPC method due to a different way of the data treatment. The pixel-by-pixel analysis in the case of FLIM does not enable fitting the decay curves due to a rather low number of photons per pixel. Thus, only the average lifetime can be calculated.
25. P. Kubát and J. Mosinger, *J. Photochem. Photobiol., A*, 1996, **96**, 93.

